P15R.2

HIGH-RESOLUTION, MOBILE, W-BAND, DOPPLER-RADAR OBSERVATIONS OF THE VERTICAL STRUCTURE OF A TORNADO NEAR ATTICA, KANSAS ON 12 MAY 2004

Howard B. Bluestein*, Christopher C. Weiss[1], Stephen Frasier and Andrew L. Pazmany[3] and Eric Holthaus[2]
University of Oklahoma, Norman, Oklahoma
University of Massachusetts, Amherst, Massachusetts

1.INTRODUCTION

Our knowledge of the vertical profile, in nature, of the windfield in tornadoes is limited by our ability to make measurements in them. Wurman and Gill (2000) constructed vertical profiles of wind and reflectivity in a tornado from mobile, X-band, Doppler radar sector scans. Bluestein et al. (2004b) described the vertical structure of a tornado from RHIs (range-height indicator) vertical cross sections made by a high-resolution, mobile, W-band Doppler radar. Real data such as those collected by Wurman and Gill (2000) and Bluestein et al. (2004b) are to be compared with large-eddy simulations of tornado-like vorrtices (e.g., Lewellen et al. 2000) in order to learn about the kinematics and dynamics of tornado structure, which furthers what we have learned in the past from laboratory models and simulations of laboratory models (Davies-Jones et al. 2001).

The purpose of this paper is to present results from another well-documented tornado dataset, collected in 2004, by a W-band radar.

2. DATA COLLECTION AND PROCESSING

The data described here were collected in the second of a series of tornadoes associated with a supercell on 12 May 2004, in south-central Kansas, near Attica, from a range of only 2 – 3 km (Figs. 1 and 2).

The data were collected by a truck-mounted, W-band Doppler radar designed and built at the Microwave Remote Sensing Laboratory (MIRSL) at the Univ. of Massachusetts at Amherst. This radar system has been used for over a decade to collect data detailing the structure of tornadoes and dust devils (Bluestein and Pazmany 2000; Bluestein et al. 2003; Bluestein et al. 2004a,b).

*Corresponding author address: Howard B. Bluestein, School of Meteorology, Univ. of Oklahoma, Norman, OK 73019; e-mail: hblue@ou.edu

Current affiliation:
[1]Texas Tech University, Lubbock, TX
[2]Columbia University, New York, NY
[3]ProSensing, Inc., Amherst, MA

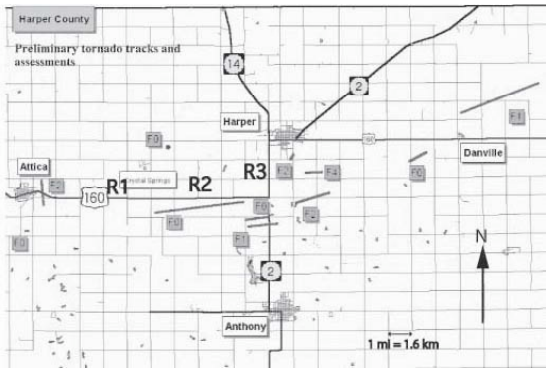

Figure 1. Tornado tracks and estimated F-scale rating of each tornado on 12 May 2004, as determined by the National Weather Service, Wichita, KS. Also shown are the three main deployment sites of the U. Mass. mobile radars (R1, R2, and R3) along the main highways.

Figure 2. The second tornado on 12 May 2004 at approximately 2003 CDT. The view is to the west from a location approximately 5 km east of Attica, KS on Highway 160 (R1 in Fig. 1). Photograph copyright H. Bluestein.

The most important characteristic of the radar is its high spatial resolution: The antenna has a half-power beamwidth of only 0.18 deg; this narrow beamwidth yields an azimuthal resolution of only 10 m at a range of approximately 3 km. The range resolution was 30 m. Data were collected out to a range of 10 km. Beyond 1.5 km, polarization diversity pulse-pair processing

(PDPP) (Pazmany et al. 1999) is employed so that the maximum unambiguous velocity is just under 80 m s^{-1}. Unfortunately, owing to a cable malfunction, only conventional pulse-pair processing was available on 12 May 2004, so that the maximum unambiguous velocity was only ±8 m s^{-1} and the data had to be manually unfolded, which was rather tedious. The velocity data were unfolded based on sector scans through the tornado just before and after a series of RHIs were collected. Boresighted video frames were used to aid in the unfolding process. Since the tornado traveled in a direction approximately normal to the radar beam (Fig. 1), it was usually easy to locate the zero isodop, which is assumed to pass approximately through the center of the vortex. Data for which the reflectivity was less than –15 dBZ were too contaminated by noise and were therefore discarded.

This study focuses on a series of ten quasi-vertical scans taken across the entire width of the tornado condensation funnel and debris cloud (Fig. 3). Fig. 3 was developed after careful analysis of both the boresighted video and the radar data, which indicated when the radar passed through the ground. Although the scans were made in approximately a vertical plane (the radar truck was not leveled exactly) and since the tornado was translating from left to right across the viewing plane, the scans were tilted slightly across the tornado. In the case of the Happy, TX tornado (Bluestein et al. 2004b) the vertical scans were also tilted slightly, but in this case the scans were tilted as result of the motion along the radar beam.

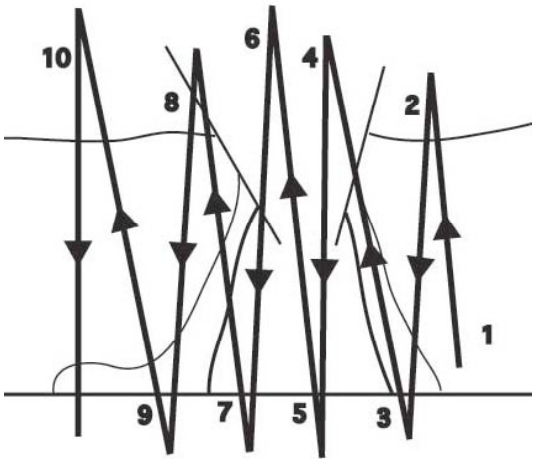

Figure 3. Schematic depicting the relationship between the quasi-vertical scans (very thick solid lines) by the U. Mass., mobile, W-band Doppler radar, through the Attica, KS tornado, when it was mature, and the visual funnel cloud (thick solid lines), opaque debris cloud (thick solid lines), and semi-transparent debris cloud (thin solid lines) from 2001:44 to 2003:27 CDT. Ground level is depicted by thick, horizontal, solid line at the bottom. Direction of scans with respect to visual features is indicated by the sense of the arrows. Scans 1, 2, 3, 4, 5, 6, 7, 8, 9, and 10 began at 2001:44, 2001:53, 2002:03, 2002:15, 2002:26, 2002:39, 2002:51, 2003:02, 2003:13, and 2003:27 CDT, respectively.

To get a larger-scale perspective of the character of the scans through the tornado, it is useful to look at a mobile, X-band, Doppler radar reflectivity image (Pazmany et al. 2003; Kramar et al., 2005) obtained close in time to that of the W-band scans, from which the relationship between the tornado and its parent storm, just before the RHIs were initiated, can be seen.

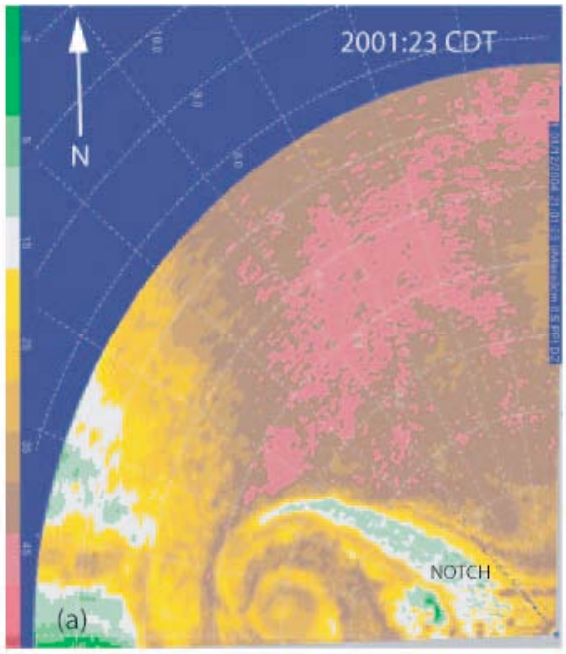

Figure 4. Storm-scale, low-elevation-angle view of the tornado near Attica, KS on 12 May 2004: Doppler radar imagery from the mobile, U. Mass., X-band, dual-polarization, Doppler radar at 2001:23 CDT. Radar reflectivity factor is shown in dBZ; color scale is shown at the left edge of the figure. Range markings are given in km and are shown every km.

The radar was located along the eastern fringe of the weak-echo notch as data collection commenced. Since little or no precipitation was falling at the radar, it is assumed that the radar must have been in the notch during data collection. The tornado was located at the ring of high reflectivity seen in the lower - center of the image, while the bulk of the precipitation in the parent storm was located to the north and northeast of the tornado.

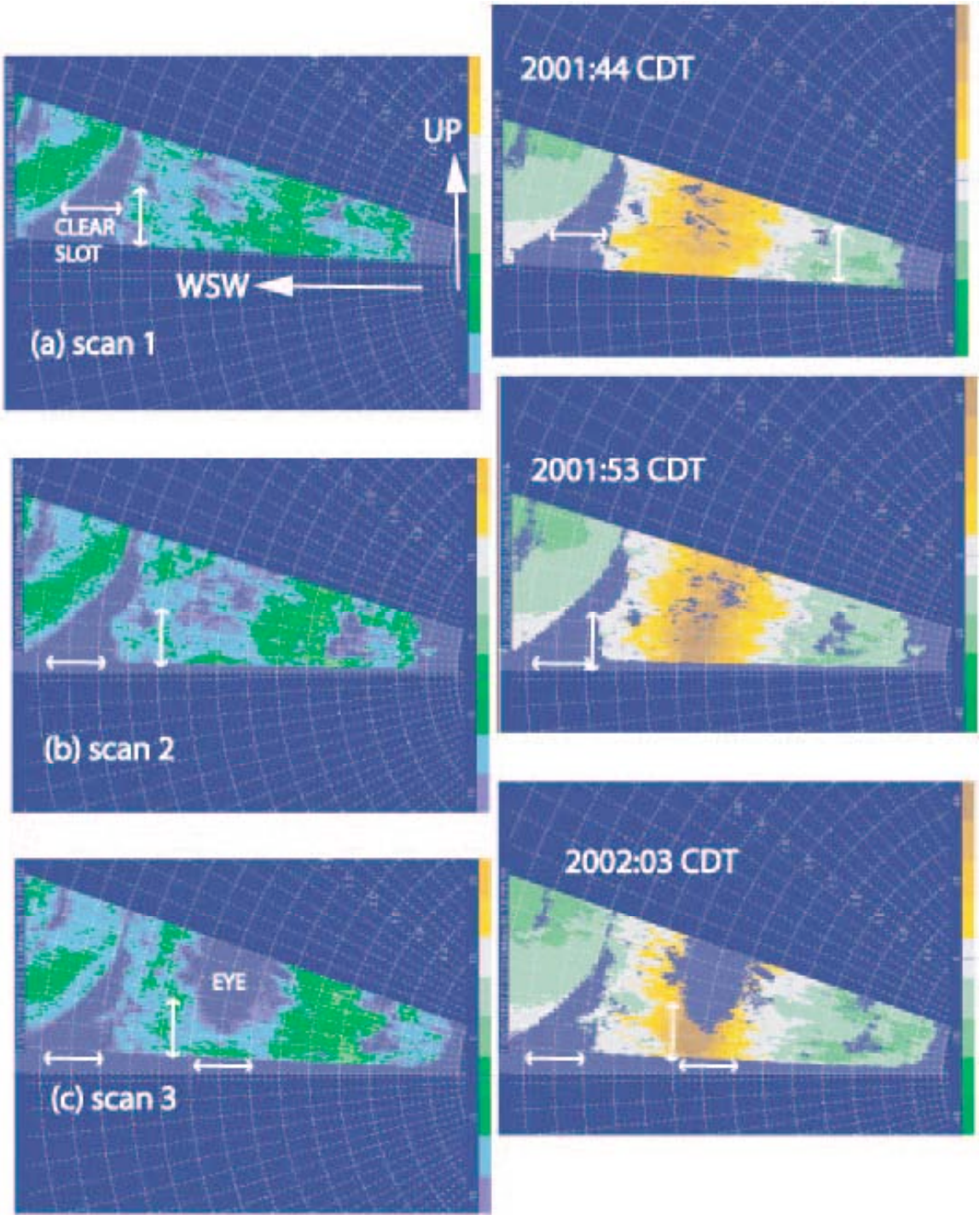

Figure 5. Quasi-vertical cross sections of W-band radar reflectivity (left panels, dBZ_e) and Doppler velocity (right panels, m s^{-1}) at (a) 2001:44, (b) 2001:53, and (c) 2001:03 CDT on 12 May 2004 through the Attica, KS tornado. Color scales for radar reflectivity (dBZ) and Doppler velocity (m s^{-1}) are shown at the right edge of each panel, respectively. Range is given in km, every 200 m. To aid the reader, white line segments with double arrows indicating 400 m are shown in each panel, for both vertical and horizontal scale. The bottom of each cross section is just above the ground level. The corresponding scan numbers sketched in Fig. 3 are identified. This figure begins with the scan through the farthest to the right of the tornado condensation funnel and debris cloud.

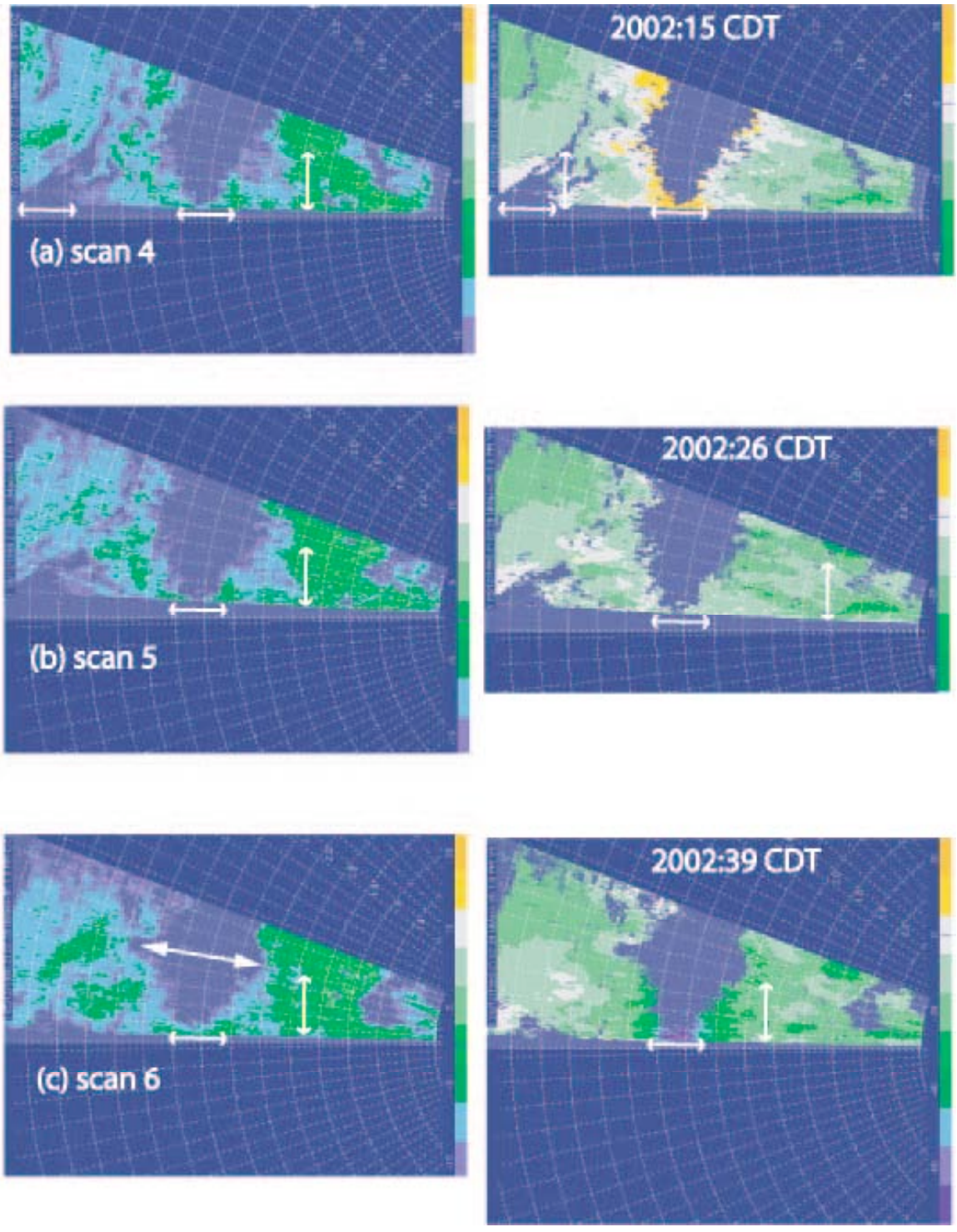

Figure 6. As in Fig. 5, but for (a) 2002:15, (b) 2002:26, and (c) 2002:39 CDT. This figure contains the scans through the center of the condensation funnel. The thick double arrow in (c) marks the bulge in the eye.

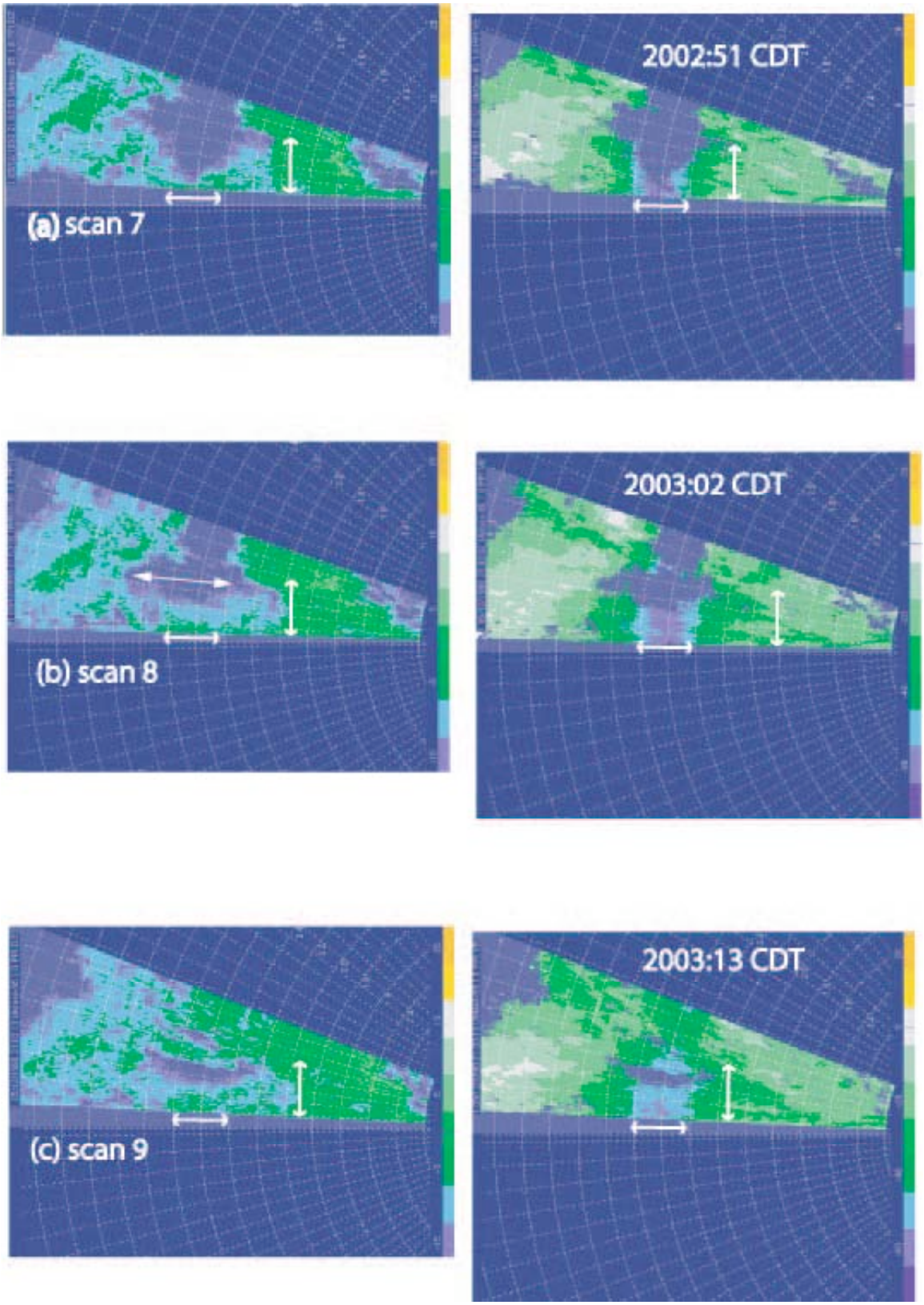

Figure 7. As in Fig. 5, but for (a) 2002:51, (b) 2003:02, and (c) 2003:13 CDT. This figure contains the scans through the left side of the condensation funnel and debris cloud. The longer double arrow in (b) marks the bulge in the eye.

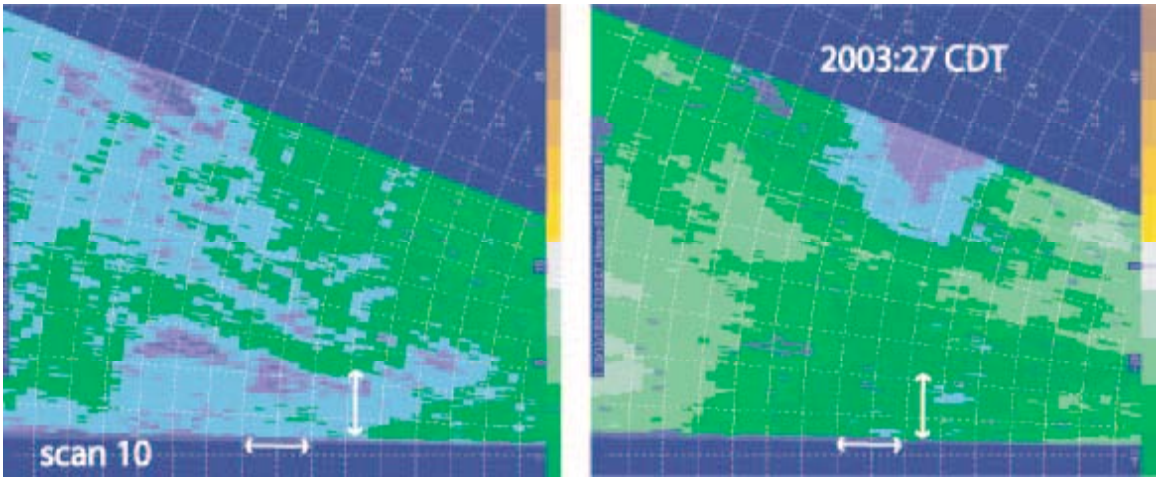

Figure 8. As in Fig. 5, but for 2003:27 CDT; the range markings are shown every 100 m; the double arrows represent 200 m. This figure represents one scan through far to the left of the condensation funnel and through the left edge of the debris cloud.

3. VERTICAL CROSS SECTIONS OF RADAR REFLECTIVITY AND DOPPLER VELOCITY

The salient features of the quasi-vertical slices through the tornado are now summarized. The "clear slot" or "notch" seen in the X-band image (Fig. 4) is evident in Figs. 5a, b, c and 6a on the north side of the tornado. The clear slot is widest near the ground, but closes up aloft at higher and higher altitudes with increasing distance to the north; it slopes radially inward from the tornado with height on its far side, but is nearly vertical on its near side.

The weak-echo eye appears first aloft in scan 3 (Fig. 5c, left panel). The strongest receding Doppler velocities are found in scan 3 (Fig. 5c, right panel), just to the right of the condensation funnel, just beyond/within the bounds of the opaque/semi-transparent debris cloud (cf. Fig. 3).

Through the center of the tornado (Fig. 6b, right panel) in scan 5, the Doppler velocities are at their minimum values overall and the weak-echo eye extends to within 10 m or so of the ground. Uncertainties about the positioning of the antenna with respect to the ground make it impossible to be more precise about how low to the ground the eye actually penetrates. The eye has a pear-shaped appearance (Fig. 6 a-c, left panel, as in Bluestein et al. (2004b) and in the simulations of Dowel et al. (2005). The diameter of the eye is greatest at around 450 – 500 m AGL. A velocity couplet indicating flow into, below and flow away from, aloft is evident on the far side of the tornado at about 400 m AGL (green-white couplet in Fig. 6b, right panel).

Beginning in scan 6 (Fig. 6c, left panel) and continuing through and including scan 8 (Figs. 7a, b, left panels), there is an outward bulge in the eye around 450 – 500 m AGL that descends to around 400 m AGL. The bulge appears solely as an arc of low reflectivity in scans 9 (Fig. 7c, left panel), and 10 (Fig. 8, left panel) just below 400 m AGL. Thus, the bulge and arc of low reflectivity are evident only through the center and south sides of the tornado. There is circumstantial evidence that the in-below, out-above couplet seen through the center of the tornado, on the far side, are associated with the bulge and arc, as scatterer-sparse air from within the eye is advected radially outward, while scatterer-rich air is advected inward underneath.

The highest approaching Doppler velocities are evident in scan 6 (Fig. 6c, right panel), near the ground and within the debris cloud. Lack of scatterers above in the eye make it impossible to know if even higher velocities were present at higher altitudes.

The elevated region of higher approaching Doppler velocity seen in scan 10 (Fig. 8, right panel) may be associated with a rear-flank downdraft (RFD). Since scans were not made to the left of scan 10, it is not known how this feature sloped to the south of the tornado.

4. VERTICAL PROFILES OF HORIZONTAL WIND

From the quasi-vertical cross sections of Doppler velocity, vertical profiles of Doppler velocity and the absolute value of Doppler velocity (Doppler wind speed) were calculated and plotted (Fig. 9). The interpretation of the profiles is made difficult because the scans were not exactly in the vertical plane, so that some of the variation with height is really an artifact, owing to variations in wind *across* the tornado.

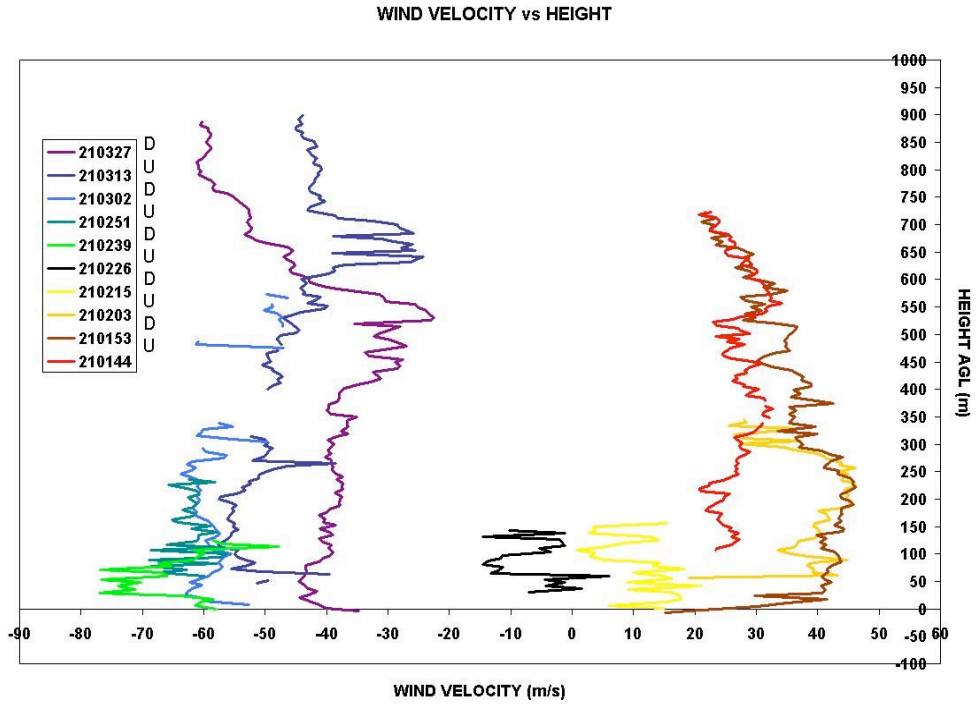

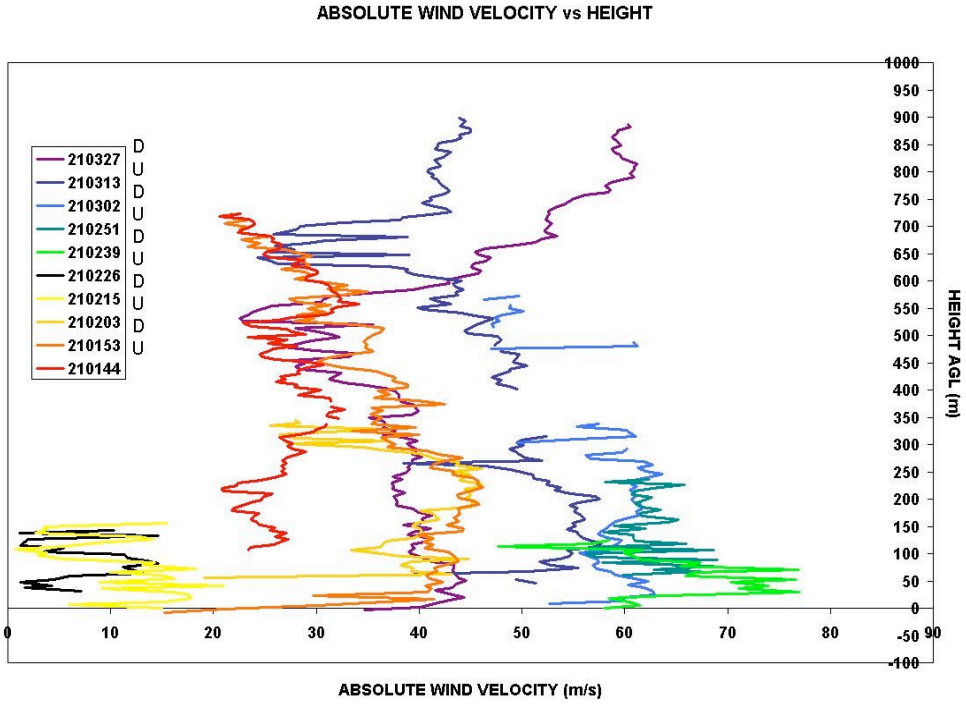

Figure 9. Variations of the Doppler (quasi-horizontal) wind component (m s^{-1}) with height (m AGL) in the Attica, KS tornado on 12 May 2004 from 2001:44 to 2003:27 CDT, when it was mature. (a) Doppler velocity (m s^{-1}) as a function of height (m AGL); (b) Absolute value of Doppler velocity (m s^{-1}) as a function of height (m AGL). The times (CST; the times in CDT are 1 h earlier) for each vertical profile are shown in the insets in the upper left in each panel; upward and downward scans are indicated by “U” and “D,” respectively.

In general, the receding Doppler velocities decreased with height above 500 m AGL. The highest approaching Doppler velocities were found around 50 m AGL. In the two scans to the most left (south) of the tornado, relatively high approaching Doppler velocities were found aloft above 600 – 700 m AGL; this relative maximum in approaching Doppler velocities slopes outward from the tornado. It may represent an RFD (cf. Fig. 8, right panel).

The absolute magnitude of Doppler velocity in general decreased with height up to about 250 m AGL by around 10% or in some instances a bit more, especially near the center of the tornado (where data are available only at low levels, underneath the weak-echo eye). In the latter case, the horizontal variation in wind speed (cf. Fig. 3) might be dominating the vertical variation and therefore the vertical profiles are not representative.

5. SECTOR SCAN ACROSS THE TORNADO

Finally, a sector scan taken across the tornado at low elevation angle, about 45 s following the series of vertical scans depicted in Figs. 5 -8, is discussed. (The scan taken just before the series of vertical scans covered only a portion of the tornado and is therefore not shown here.) The tornado at this time was in its dissipating stage; the condensation funnel became ropelike in appearance (not shown) as is typical in the life of many tornadoes (Davies-Jones et al. 2001).

The reflectivity image (Fig. 10a) is similar to that of Bluestein et al. (2003) in that a spiral pattern with only a diffuse eye is evident. The maximum and minimum in the Doppler velocity couplet associated with the tornado (Fig. 10b) are spaced apart by about 200 - 250 m; thus, the core radius of the tornado was approximately 100 - 125 m. The maximum Doppler velocity was approximately 55 m s^{-1} in the approaching direction.

6. SUMMARY AND CONCLUSIONS

High-resolution W-band Doppler-radar data collected in s supercell tornado were analyzed with the aid of boresighted video images. It was found that the tornado was associated with a pear-shaped weak-echo eye, which penetrated to within 10 m or so of the ground at the center.

Evidence was found that scatterer-free air was advected outward by a horizontal circulation about 450 – 500 m AGL. The clear-slot or notch sloped upward to the north (toward the parent storm); its far side flared inward (toward the tornado) with height and was widest near the ground; the side closest to the tornado was nearly vertical. Highest Doppler velocities overall were found below 500 m; the highest approaching Doppler velocities were found around 50 m AGL.

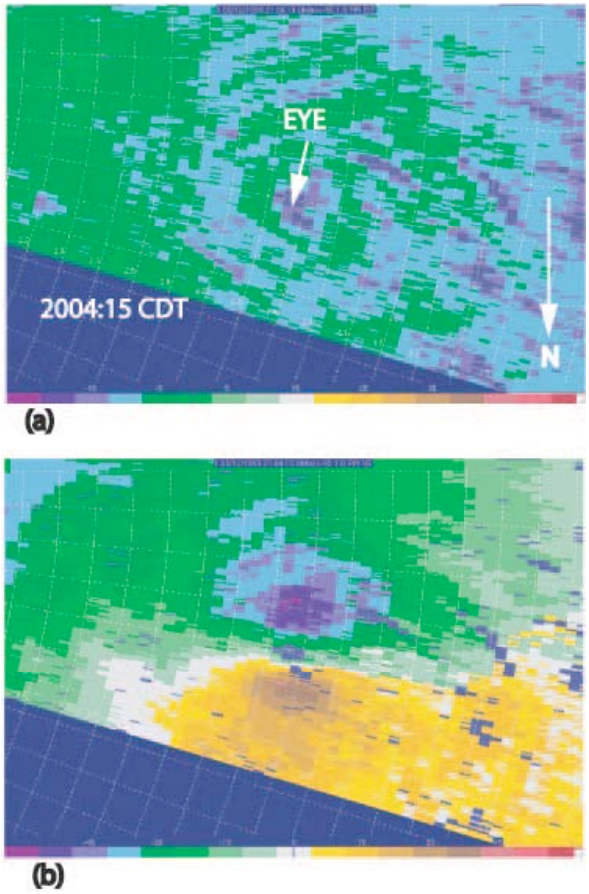

Figure 10. Small-scale, constant elevation-angle view of the Attica, KS tornado on 12 May 2004, while it was dissipating): Doppler radar imagery from the mobile, U. Mass., W-band, Doppler radar at at 2004:15 CDT. (a) Radar reflectivity in dBZ_e; (b) Doppler velocity in m s^{-1}. Color scales for radar reflectivity and Doppler velocity are shown at the bottom edge of each panel in (a) and (b), respectively. Range markings are shown in km, every 100 m.

Future data-collection in tornadoes should be conducted in conjunction with other radars scanning the entire parent storm. The W-band radar system is expected to be subjected to a major overhaul before spring, 2006, so that it will be possible to scan more rapidly and to examine the data more easily in real time.

ACKNOWLEDGMENTS

This research was funded by NSF grants ATM-ATM-0241037 to OU and ATM-0000592 to U. Mass. Support was also provided by the School of Meteorology at the University of Oklahoma (OU). The second author operated the radar in the field. The authors thank Mark Laufersweiler (OU) for his assistance with computer-related issues.

REFERENCES

Bluestein, H. B., and A. L. Pazmany, 2000: Observations of tornadoes and other convective phenomena with a mobile, 3-mm wavelength, Doppler radar: The spring 1999 field experiment. *Bull. Amer. Meteor. Soc.*, **81**, 2939-2951.

_____, C. C. Weiss, and A. L. Pazmany, 2004a: Doppler-radar observations of dust devils in Texas. *Mon. Wea. Rev.*, **132**, 209 – 224.

_____, C. C. Weiss, and A. L. Pazmany, 2004b: The vertical structure of a tornado near Happy, Texas, on 5 May 2002: High-resolution, mobile, W-band, Doppler radar observations. *Mon. Wea. Rev.*, **132**, 2325 – 2337.

_____ , W.-C. Lee, M. Bell, C. C. Weiss, and A. L. Pazmany, 2003: Mobile-Doppler-radar observations of a tornado in a supercell near Bassett, Nebraska on 5 June 1999. Part II: Tornado-vortex structure. *Mon. Wea. Rev.*, **131**, 2968 – 2984.

Davies-Jones, R. P., R. J. Trapp, and H. B. Bluestein, 2001: Tornadoes and tornadic storms. *Severe Convective Storms* (C. Doswell III, ed.), Meteor. Monogr., **28**, no. 50, Amer. Meteor. Soc., 167-221.

Dowell, D. C., C. R. Alexander, J. M. Wurman, and L. J. Wicker, 2005: Reflectivity patterns and wind-measurement errors in high-resolution radar observations of tornadoes. *Mon. Wea. Rev.* , **133**, 1501 – 1524.

Kramar, M. R., H. B. Bluestein, A. L. Pazmany, and J. D. Tuttle, 2005: The “Owl Horn” radar signature in developing Southern Plains supercells. *Mon. Wea. Rev.* , **133**, 2608 – 2634.

Lewellen, D. C., W. S. Lewellen, and J. Xia, 2000: The influence of a local swirl ratio on tornado intensification near the surface. *J. Atmos. Sci.*, **57**, 527-544.

Pazmany, A. L., J. C. Galloway, J. B. Mead, I. Popstefanija, R. E. McIntosh, and H. B. Bluestein, 1999: Polarization diversity pulse pair technique for millimeter-wave Doppler radar measurements of severe-storm features. *J. Atmos. Ocean. Tech.*, **16**, 1900-1911.

_____, F. J. Lopez, H. B. Bluestein, and M. Kramar, 2003: Quantitative rain measurements with a mobile, X-band, polarimetric Doppler radar. Preprints, *31st Conf. on Radar Meteor.*, Seattle, WA, Amer. Meteor. Soc., 858 – 859.

Wurman, J., and S. Gill, 2000: Finescale radar observations of the Dimmitt, Texas (2 June 1995), tornado. *Mon. Wea. Rev.*, **128**, 2135-2164.